Available online at http://ijcpe.uobaghdad.edu.iq and www.iasj.net
Iraqi Journal of Chemical and Petroleum Engineering
Vol.23 No.4 (December 2022) 59 – 69
EISSN: 2618-0707, PISSN: 1997-4884

Mathematical Modeling and Kinetics of Removing Metal Ions from Industrial Wastewater

Nizar A. Jawad and Tariq M. Naife

Chemical Engineering Department – College of Engineering – University of Baghdad

Abstract

The study's objective is to produce Nano Graphene Oxide (GO) before using it for batch adsorption to remove heavy metals (Cadmium Cd^{+2}, Nickel Ni^{+2}, and Vanadium V^{+5}) ions from industrial wastewater. The temperature effect (20-50) °C and initial concentration effect (100-800) mg L^{-1} on the adsorption process were studied. A simulation aqueous solution of the ions was used to identify the adsorption isotherms, and after the experimental data was collected, the sorption process was studied kinetically and thermodynamically. The Langmuir, Freundlich, and Temkin isotherm models were used to fit the data. The results showed that Cd, Ni, and V ions on the GO adsorbing surface matched the Langmuir model with correlation coefficients (R^2) of 0.999. Kinetic models studied showed that a pseudo-second-order model was followed and thermodynamically, the process was exothermic due to ΔH negative, the reduction in randomness because of negative ΔS. additionally, spontaneous adsorption of metal ions was ΔG negative values influenced.

Keywords: Nano Graphene Oxide; Heavy Metal; wastewater; Langmuir model; Pseudo-second-order; Thermodynamic study.

Received on 30/06/2022, Accepted on 25/08/2022, Published on 30/12/2022

https://doi.org/10.31699/IJCPE.2022.4.8

1- Introduction

With the expansion of industry and human activity, there are more heavy metals in industrial wastewater. Mining, plating and electroplating, batteries, insecticides, metal rinse operations, rayon, tanning, bioreactors of fluidized bed, the industry of textile, metal smelting, applications of electrolysis, a paper production, as well as petrochemicals, are some examples. The wastewater from oil refineries is the most significant of these [1,2]. Heavy metal-contaminated water enters the ecosystem, harming both human health and the environment. Because heavy metals do not biodegrade [3] and may cause cancer, as well as their inappropriate concentration in water, which may have serious negative effects on the health of living things [4,5].

Industrial wastewater effluent may include a set of heavy metals, like Zinc (Zn), Mercury (Hg), Iron (Fe), Lead (Pb), Arsenic (As), silver (Ag), Chromium (Cr), Boron (B), Manganese (Mn), Calcium (Ca), Molybdenum (Mo), Cobalt (Co), Antimony (Sb), and others may be found in industrial effluent. The most prevalent heavy metals in effluent from oil refineries are Cadmium (Cd), Nickel (Ni), and Vanadium (V). Based on the Table **1** highlights Ni, Cd, and V ions, emphasizing their main sources, health consequences, and the allowable level in drinking water.

Conventional approaches for removing heavy metal pollution from wastewater include precipitation via coagulation and flocculation [7], electrochemical purification [8], membrane separation [9], and adsorption [10,11]. Adsorption is the most promising of these technologies because of its low cost, high efficiency, versatile design, and ease of operation. Nanomaterials are the adsorbent in the majority of typical adsorption systems because of their unique properties like a specific surface area is high, a large number of binding sites for the adsorbates to be adsorbed, numerous functional groups, and appropriate pore size, This makes them appealing adsorbents for the treating industrial wastewater polluted with heavy metals [12,13].

The GO has exceptional adsorption qualities, particularly in liquid-solid systems, according to several studies. Its structure demonstrates the presence of oxygen groups in the aromatic ring, such as carbonyl, carboxyl, and hydroxyl groups, which makes it highly hydrophilic and gives the GO a high capacity for adsorption of metal ions pollutants because of its high surface area and ability to disperse in water [14].

GO is often manufactured by oxidative exfoliation of natural graphite using the well-known Hummers technique [15,16].

In this research, GO was prepared using methods reported in the literature [17] and also studied the influence of initial concentration and temperature on the removal of heavy metal ions from wastewater by batch adsorption process. as well as Various models were used to assess the adsorption isotherm, kinetics, and thermodynamics at the solid-liquid interface.

Corresponding Authors: Name: Nizar A. Jawad, Email: nizar.jawad1607m@coeng.uobaghdad.edu.iq, Name: Tariq M. Naife, Email: tariq.mohammed@coeng.uobaghdad.edu.iq

Table 1. Typical of the Key Heavy Metals Occurring in Industrial Wastewater and their Origins, as well as the Health Risks Caused by Inadequate Levels and the Authorized Amounts in Drinking Water According to the Guidelines of the (WHO) [5]

Heavy metal ions	Major sources	The most impacted organ and system	Permitted quantities (µg)
Cadmium (Cd)	Metal refineries, batteries, paints, the steel and plastic industries, and rusted galvanized pipes.	The bones, liver, kidneys, lungs, testes, brain, immune system, and cardiovascular system are all affected.	3
Nickel (Ni)	Stainless steel and nickel alloy production.	Lung, kidney, gastrointestinal distress, pulmonary fibrosis, and skin.	70
Vanadium (V)	flue dust from smokestacks of ship boiler, crude oil	toxic element, Green tongue, cramps, diarrhea, and neurological	100

2- Experimental

2.1. Materials

Powder of Natural Graphite, 99% purity, Glentham Life Sciences L.td Co. Hydrochloric acid HCl (35-38% concentration, BHD Laboratory, Germany). Sulphuric acid H_2SO_4 (98% concentration, Sigma-Aldrich, India). Hydrogen peroxide H_2O_2 (30% concentration, Pubchem, Germany). Potassium permanganate powder $KMnO_4$ (Fisher Scientific, India), Sodium hydroxide NaOH (98% concentration, SDFCL, India), and Deionized water (DI water).

2.2. Synthesis of Nano graphene oxid GO

GO was prepared by modifying the Hummers technique [18]. Graphite powder (1.0 g) and concentrated H_2SO_4 (24 ml) were poured into an ice bath and agitated at 200 rpm by using a Hotplate Magnetic Stirrer (Labtech LMS-1003/Korea), followed by the gradual addition of $KMnO_4$ (3.0 g) to keep a temperature below 10°C. The reaction system was then placed in a 40°C Paraffin-oil bath and aggressively stirred (300 rpm) for about 30 min. After adding 50 ml of DI water to the solution, it was stirred for 15 min at 95°C. Dropwise addition of 5 ml H_2O_2 followed by 150 ml DI water. The solution's transformation from dark brown to yellow-brown indicates that the graphite has oxidized. The suspension was filtered and washed with (150 ml) of a 1:9 HCl aqueous solution with metal ions removed. The remaining acidic or metallic substances were then rinsed away with 1 L of water. The resulting GO dispersion was poured into 300 ml of water and ultrasonicated at 40 kHz frequency for 0.5 hr. The GO dispersion was then centrifuged for one hour at 5000 rpm to eliminate any un-exfoliated particles. The resultant substance was then dried at 60°C for 24 hr to produce GO.

2.3. Characterization

The X-ray diffraction XRD analysis was the most important test which is performed to establish the existence of GO and to learn about its crystalline properties, where the effective production of the GO at the peak 2θ range of 10-12 degrees [18] The GO exhibited a very significant peak at 2θ = 10.92° as shown in Fig. **1** A.

Fourier-transform infrared spectrometer to analyze the morphology of GO (FTIR; Thermo Scientific inc., NICOLET iS10, Boston, MA, USA) shows peaks corresponding to oxygen-containing functional groups, the prominent peak between 3403.27 and 2925.2 cm^{-1} is due to hydroxyl O-H stretching, and the absorption peak at 2344.97 cm^{-1} is due to the C=O bond. That result shows that GO was produced [19], as shown in Fig. **1** B.

Scanning electron micrographs SEM (Gemini SEM 500, ZEISS, Germany) were used to perform thorough morphological examinations, where the graphite oxidation rate is indicated by its crystallization. The photo shows that GO is composed of randomly aggregated and thin folded sheets with surface creases and folds [20], as shown in Fig. **1** C.

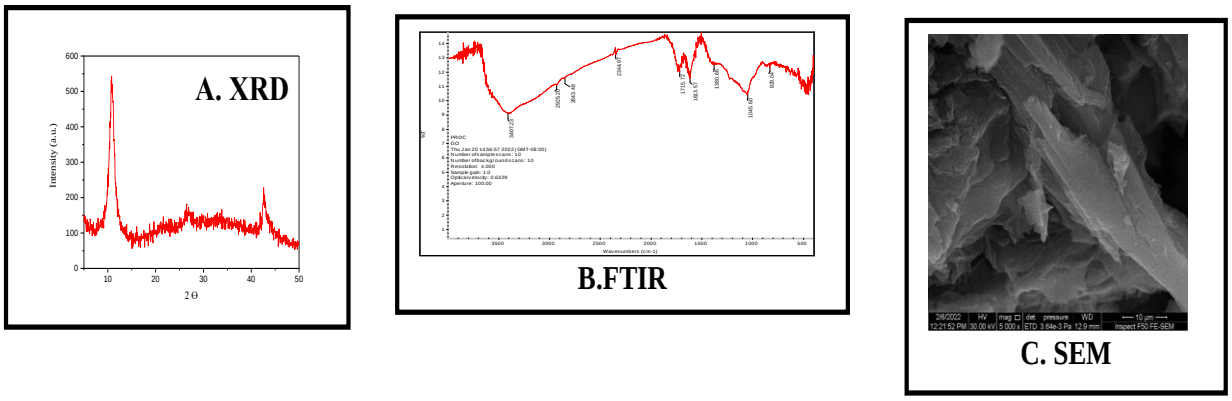

Fig. 1. A. XRD, B. FTIR, C. SEM for GO

2.4. Adsorption capacity of heavy metal ions in batch on GO

Utilizing simulated solutions created by diluting the stock solution to the required concentration in a water bath shaker with deionized water, adsorption tests were performed. To avoid spillage during the shaking operation, 100 mL of an aqueous solution containing heavy metals (Cd^{+2}, Ni^{+2}, and V^{+5}) were placed in 150 mL glass flasks and tightly covered in aluminum foil. The HCl (0.1 M), and NaOH (0.1 M) solutions were utilized to control the solution's acidic properties. Furthermore, the specified amounts of adsorbent GO were added to the heavy metals aqueous solution. The treatment technique begins by altering the temperature (20-50) °C and the starting concentration within the range of (100-800) mg L^{-1}, maintained under optimal operating conditions (pH= 7.5, Time t= 150 min, rpm= 375, 100 mg of GO) [21,22]. When the timer runs out, the shaker (Thermo Scientific MaxQ SHKE7000 Benchtop, Model 4303\ Germany) is switched off, the flasks are removed, and the samples are filtered using Filter Paper. The Atomic absorption spectrophotometer AAS (AAS SensAA GBC \ UK) is used to measure the concentration of residual heavy metals and the percentage of removal (%R), as well as the capacity of the adsorbent for batch adsorption (q_e), after the adsorbent material has been separated from the solution, using Equations (1) and (2), respectively.

$$\%R = \frac{Ci-Cf}{Ci} \times 100 \quad (1)$$

$$q_e = \frac{V}{m} \times (Ci - Cf) \quad (2)$$

Where R: denotes the percentage of heavy metal ions removed, q_e: denotes the adsorption capacity of adsorbent media ($mg.g^{-1}$), Ci and Cf: denote the initial and the end concentrations of heavy metal ions, respectively (mg L^{-1}), m: denotes the mass of adsorbent used for adsorption (g), and V: denotes the volume of solution (L).

2.5. Study isotherm, Kinetic, and Thermodynamic of the Adsorption process

As an adsorbent, 100 mg of GO was added to 100 mL. of aqueous solutions containing Cd, Ni, and V at a set starting concentration of (100-800) mg L^{-1} and temperature (20-50) °C to perform the experiments for the adsorption kinetics investigation. The samples were gathered, and the AAS technique was used to calculate the concentrations of Cd, Ni, and V in the aqueous solutions; under ideal circumstances. Equation (3) was used to calculate the heavy metal ion's adsorption capacity at time t (q_t) expressed in mg g^{-1} [19].

$$q_t = \frac{V}{m} \times (C_i - C_e) \quad (3)$$

Where: C_i (mg L^{-1}) is the initial concentration of each ion and C_e (mg L^{-1}) is the equilibrium adsorbed concentration, V is the volume (L) of the solution of the respective ion and m is the mass of adsorbent (g).

3- Result and Discussion

3.1. Adsorption performance

a. Temperature Effect (T)

The impact of removing temperature on the efficiency for Cd, Ni, and V ions using GO in a batch mode adsorption unit is shown in Fig. **2** under optimal conditions. At the changing temperature (20-50) °C, the maximum removal is achieved at the lowest temperature, suggesting an inverse relationship between temperature and adsorption efficiency for all heavy metals tested and the adsorbent (GO) applied. This proves that the adsorption was an exothermic process, which indicates that as the temperature rises, the bonds connecting the functional groups present in the active sites spread across the surface of GO with Cd, Ni, and V ions break down, allowing the material to be released and returned to the solution, thereby decreasing the removal efficiency [19]. The highest removal of metal ions was seen at 20 °C where the adsorption capacity is decrease with an increase the temperature, after which adsorption reduced steadily with increasing temperature until it reached its lowest value.

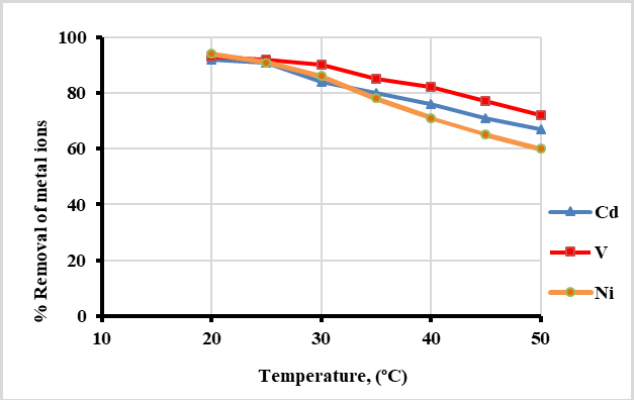

Fig. 2. Temperature Effect on % Removal of Metal Ions

b. Effect of Initial Concentration (C_i)

The influence of the starting concentration on the heavy metal adsorping process within the range of (100-800) mg.L^{-1} for Cd, Ni, and V under optimal circumstances for the remainder of the other design, as shown in Fig. **3**. The data collected demonstrate an inverse link between the two variables. For all heavy metal ions and adsorbent materials, the percentage removal falls as the initial concentration value rises [23]. There is no change in the surface area of the GO, this indicates that there are a limited number of ions that may be adsorbable on the surface of the adsorbent. Because the volume of the solution remains constant, increasing the contaminant concentration means increasing the ions of those metals, implying that heavy metal ions compete for the same amount of active sites on the adsorbent's surface [21]. As a consequence, fewer ions will be adsorbed and more heavy metal ions will be present in the contaminated

solution, decreasing the treatment's effectiveness. The highest adsorption capacity at C_i 100 mg L^{-1} and the lowest at C_i 800 mg L^{-1}.

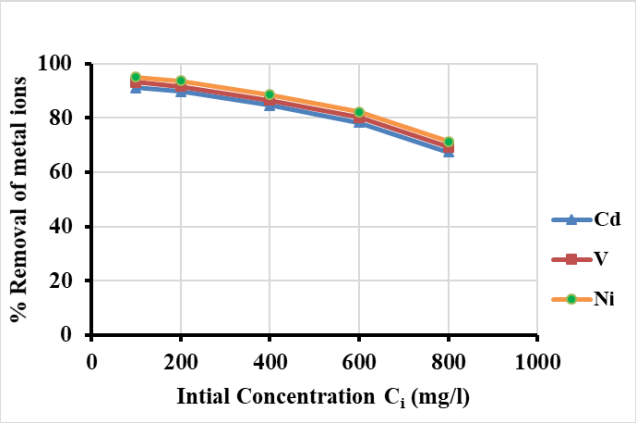

Fig. 3. Initial Concentration C_i Effect on % Removal of Metal Ions

3.2. Adsorption Isotherm

One may ascertain the connection between the concentration of the adsorbate and the amount of adsorption on the surface of the adsorbent at a constant temperature by measuring the adsorption isotherm of the ions from an aqueous solution on the GO. To calculate GO's ability to adsorb Cd^{+2}, Ni^{+2}, and V^{+5} ions from an aqueous solution. To establish the best model fit and calculate adsorption, the experimental isotherm data were examined using models. each model's parameters. The used models were Langmuir, Freundlich, and Temkin. The models were used to replicate and comprehend the method by which Cd, Ni, and V ions adsorb on the graphene sheets constituting the Nano Graphene Oxide (GO) structure. These models are represented by the following equations, which also explain the significance of each parameter.

a. Langmuir Model

It is predicated on the idea that when the adsorbed solute forms a monolayer, the adsorbent has consistent adsorption energy at a constant temperature. Expresses the linear form Equation (4) [24]:

$$\frac{1}{q_e} = \frac{1}{q_{max} K_L} \frac{1}{C_e} + \frac{1}{q_{max}} \quad (4)$$

Where q_e: capacity of equilibrium adsorption (mg g^{-1}), C_e: equilibrium adsorbed concentration (mg L^{-1}), K_L: Langmuir constant, expressed the binding sites (L mg^{-1}) and q_{max}: the capacity of maximum adsorption (mg g^{-1}).

b. Freundlich Model

According to this model, adsorption takes place on a heterogeneous surface with homogeneous energy across several layers, and Equation (5) may be used to linearly characterize this process [23]:

$$q_e = K_F C_e^{\frac{1}{n}} \quad (5)$$

Where: q_e: the amount adsorbed per unit mass of adsorbent (mg g^{-1}). K_F: The Freundlich constant represents the measured adsorption capacity [(mg g^{-1}). $(mg^{-1})^{1/n}$]. n: intensity of adsorption (-).

c. Temkin Model

The number of active sites on the adsorbent material's surface was proportional to the number of metal ions adsorbed. We can calculate the adsorption energy as well as the interactions between ions and GO using Temkin's model. According to Temkin's model, adsorption is characterized as a uniform distribution of binding energy up to the maximum amount [23], which implies that the reduction in heat of absorption is linear rather than logarithmic as in Freundlich's equation [24]. Use Equation (6) to apply the Temkin isotherm:

$$q_e = \frac{RT}{b} \ln K_T + \frac{RT}{b} \ln C_e \quad (6)$$

Where: q_e: equilibrium capacity of adsorption (mg g^{-1}), R: ideal gas constant (8.3144 J $mol^{-1}.°K^{-1}$), Ce: equilibrium adsorbed concentration (mg L^{-1}), T: Absolute temperature (°K), K_T: binding constant for Temkin isotherm equilibrium (L mol^{-1}), b: Temkin isotherm constant related to the heat of adsorption (J mol^{-1}).

Table **2** shows the constant amount of the Langmuir, Freundlich, and Temkin isotherms, while Fig. **4** to Fig. **6** show these isotherms for GO adsorption of the heavy metals cadmium, nickel, and vanadium, respectively.

These findings demonstrate that the experimental results exhibit the following degree of model conformity: According to the magnitude of the correlation coefficient (R^2), Langmuir is superior to Temkin and Freundlich for the metals Cd, Ni, and V. The metal ions Cd, Ni, and V adsorption using GO as adsorbents match the Langmuir isotherm more closely than other models due to the correlation coefficient (R^2) is high. Depending on the value of the separation factor, the adsorption process is chosen. Adsorption occurs on a monolayer surface with a particular number of identical patches, according to this theory. Adsorption is a physical phenomenon that occurs on a heterogeneous surface.

Table 2. Constant Values of Langmuir, Freundlich and Temkin Isotherms for Cadmium, Nickel and Vanadium Ions Adsorption Using GO

Metal	Langmuir				Freundlich			Temkin		
	q max	KL	RL	R^2	KF	n	R^2	BT	KT	R^2
Cd	653.595	0.01821	0.1207	0.99985	32.831224	1.88214	0.95213	137.888	0.1997	0.9914
Ni	581.3953	0.03955	0.0595	0.99743	51.77876	2.13196	0.95712	127.963	0.3853	0.95712
V	621.1180	0.02546	0.0894	0.99943	40.4979	1.98428	0.95364	134.205	0.2644	0.992

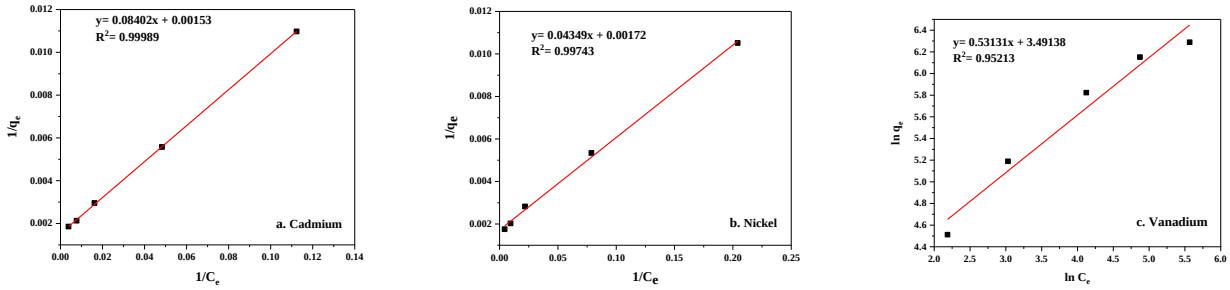

Fig. 4. Langmuir Isotherm for (a. Cadmium, b. Nickel, and c.Vanadium) Adsorption by GO

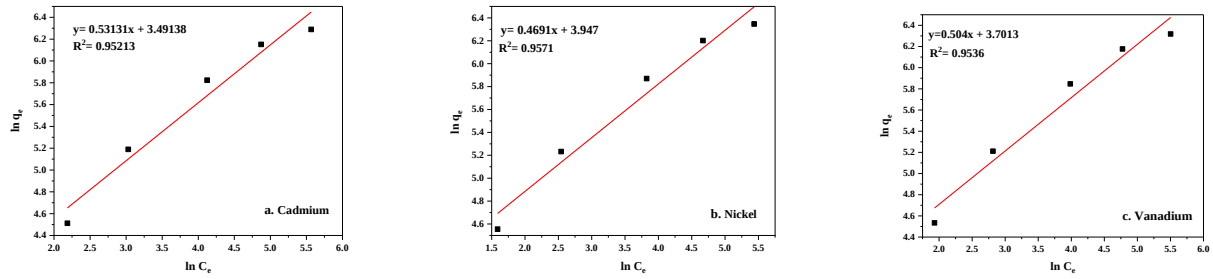

Fig. 5. Freundlich Isotherm for (a. Cadmium, b. Nickel, and c.Vanadium) Adsorption by GO

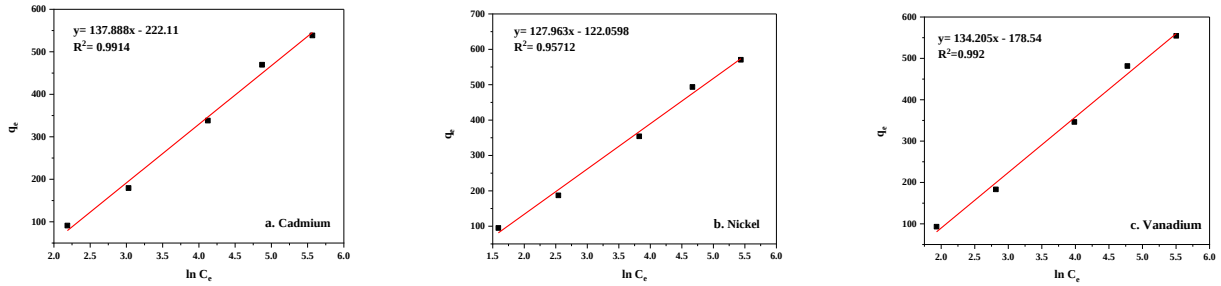

Fig. 6. Temkin Isotherm for (a. Cadmium, b. Nickel, and c.Vanadium) Adsorption by GO

3.3. Adsorption Kinetics

It is a mathematical representation in the shape of a curve or a straight line that reflects the rate at which adsorbate ions were released from the medium of the aqueous or captured by the solid phase represented by the adsorbent surface under given operating conditions. As a consequence, a kinetic investigation is required to Analyze the effectiveness and mechanics of the adsorption process. The pseudo-first-order model, pseudo-second-order model, Elovich model, and intra-particle diffusion model are the most important kinetic models for modeling the adsorption process, and they were used to analyze the experimental results in this study [25,26].

a. Pseudo First Order Model

The Lagergren model is named after Swedish scientist Sten Yngve Dennis Lagergren, who suggested it in 1898. This model implies that adsorption occurs in a single layer between the liquid and solid phases at the adsorption surface. Equation (7) demonstrates how to formally describe this model:

$$\frac{dq_t}{dt} = k_1(q_e - q_t) \quad (7)$$

Where q_t: is adsorbate adsorbed on to adsorbent at time t (mg g^{-1}), q_e : is capacity of equilibrium adsorption (mg g^{-1}), and k_1: is rate constant (min^{-1}).

By integrating Equation (7) at the boundary conditions of t = 0 to t = t and q_t = 0 to q_t = q_t provided the linear form for this model, which is defined in Equation (8) and may be shown by charting ln(q_e - q_t) versus t. The equilibrium constants k_1 and ln q_e are the slope and intercept, respectively.

$$ln\,(q_e - q_t) = ln\,q_e - k_1 t \quad (8)$$

b. Pseudo-Second Order Model

The dissolved ions' adsorption from an aqueous solution that results from interactions between physicochemical systems for the adsorbate (liquid phase) and the adsorbent is best modeled by the pseudo-second-order model (solid phase). In this model, it is a presumption that the number of active sites that are accessible on the surface of the adsorbent medium is related to the rate of adsorption. Equation (9) is the formula for this model in mathematics.

$$\frac{dq_t}{dt} = k_2(q_e - q_t)^2 \quad (9)$$

Where q_e : is the cyanide ion quantity adsorbate per unit mass of adsorbent at equilibrium (mg g^{-1}), q_t : is the cyanide ion quantity adsorbate per unit mass of adsorbent at any time (mg g^{-1}), t : is the time (min), and k_2 : is the first second-order rate constant (g mg $^{-1}$ min^{-1}).

Equation (10), which may be depicted as a linear relationship by plotting t /q_t vs t, was produced by integrating equation (9) at the boundary conditions from t= 0 to t= t and q_t= 0 to q_t= q_t and rearranging the components. The slope and intercept are represented by $1/q_e$ and $1/k_2{q_e}^2$, respectively.

$$\frac{t}{q_t} = \frac{1}{k_2{q_e}^2} + \frac{1}{q_e}t \quad (10)$$

c. Elovich Model

In 1934, the Belarusian physicist Jakow Borissowitsch Zeldowitsch and the Russian scientist S. Z. Roginsky developed this concept, which became known as the Elovich model. This model claims that the adsorption rate decreases exponentially as the quantity of adsorbent adsorbed on the adsorption surface rises. Consequently, Equation (11) may be used to numerically represent this model:

$$\frac{dq_t}{dt} = \alpha e^{-\beta q_t} \quad (11)$$

Where α: the rate of adsorption initial (mg g^{-1} min^{-1}), and β is the desorption constant.

Equation (12) produce by integrating Equation (11) at the boundary conditions of t= 0 to t= t and q_t= 0 to q_t= q_t and arranging the terms provided the linear form for this model:

$$q_t = \frac{1}{\beta}\, ln\left(\frac{1}{\alpha\beta} + t\right) + \frac{1}{\beta}\, ln(\alpha\beta) \quad (12)$$

Equation (12) can be written in the following equation (13) form, When the system is closer to an equilibrium state, $t \gg (\alpha\beta)^{-1}$:

$$q_t = \frac{1}{\beta}\ln t + \frac{1}{\beta}\ln(\alpha\beta) \quad (13)$$

By plotting qt against t we can represent a linear relationship, the $(\beta)^{-1}$ and (β^{-1} ln αβ) are the slop and intercept respectively.

d. Intra-Particle Diffusion Model

This model was established by W.J. Weber and J.C. Morris in 1963, and it was used to compute the rate-limiting step. According to the model's assumptions, in four stages, the solute is transferred from the solution to the adsorption surface. If adsorbent material is present in the solution, the first step is the mass transfer (bulk movement), or the transfer of solute molecules. This procedure is quite rapid. The subsequent phase is film diffusion, in which the solute moves inside the border layer of the adsorbent material. The other step is surface diffusion, which involves the dispersion of solute particles and their migration towards the pores of the adsorption surface. The subsequent phase is pore diffusion, which consists of the adsorption of solute molecules to active sites on the adsorption surface. The formula (14) gives the mathematical equation that characterizes the intra-particle diffusion paradigm.

$$q_t = k_p\sqrt{t} + C \quad (14)$$

Where k_p: rate constant ($mg\ g^{-1}\ min^{-0.5}$), and C: boundary layer thickness. The values of C determine the boundary layer effect—the higher values, the greater the effect.

When plot q_t against $\sqrt{t}$, The slope of the straight line indicates the constant time k_p Considering that the constant C can be determined from the intercept, the equation is linear.

Table **3** includes the amount of the parameters of the four models of kinetic that were used to evaluate the study's results. Fig. **7** to Fig. **10** illustrate the practical data from the kinetic research on Cd, Ni, and V ions removal from aqueous solutions using GO (i.e. Pseudo First Order, Pseudo Second Order, Elovich, and Intra-Particle Diffusion models).

The following kinetic model is most suited to reflect the data, according to the correlation coefficient values (R^2) of the outcomes for each metal ion:

For Cd^{+2}, Pseudo second order model > Pseudo first order model > Elovich model > Intra-particle diffusion.

For Ni^{+2}, Pseudo second order model > Pseudo first order model > Intra-particle diffusion > Elovich model.

And For V^{+5}, Intra-particle diffusion > Pseudo first order model > Pseudo second order model > Elovich model.

The Cd^{+2} and Ni^{+2} finding may be explained by the fact that, by the pseudo-second-order model and the pseudo-first-order model, The mount of metal ions adsorbed was inversely correlated with the number of active sites on the surface of the adsorbent material. According to the intra-particle diffusion model, the V^{+5} finding may be explained by the extremely quick movement of solute molecules and ions within the border layer of the adsorbent material, as well as by the surface diffusion of those solute particles towards the adsorption pores.

The results of the kinetic investigation, with a low correlation coefficient (R^2), were in agreement with the Elovich model, which postulates a gradual concentration-dependent decline in the amount of Cd, Ni, and V ions adsorbed.

Table 3. Constant Values of Pseudo-First-Order, Pseudo-Second-Order, Elovich, and Intra Particle-Diffusion Models for Cadmium, Nickel, and Vanadium Ions Adsorption Using GO

Metal	Pseudo-first-order model			Pseudo-second-order model			Elovich model			Intra-particle diffusion		
	qe	k1	R2	Qe	k2	R2	α	β	R2	kp	C	R2
Cd	132.5407	-0.000205	0.9746	100.8065	0.00054	0.9783	14.477	0.053	0.9584	6.9489	10.2845	0.911
Ni	88.3221	-0.000159	0.9147	111.9821	0.00031	0.9220	12.584	0.049	0.8732	7.7065	4.9632	0.8799
V	189.614	-0.000214	0.9432	118.0638	0.00019	0.8747	10.469	0.050	0.8727	7.7582	-0.4934	0.9481

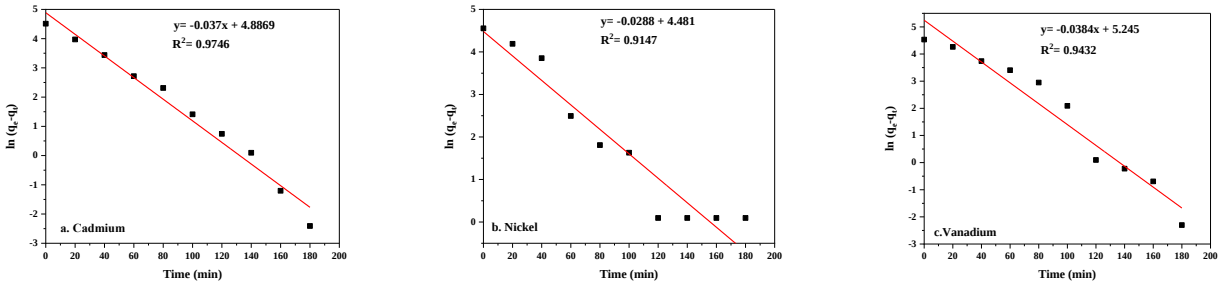

Fig. 7. Pseudo First Order Kinetic Model of GO for (a. Cadmium, b. Nickel, and c. Vanadium) Adsorption

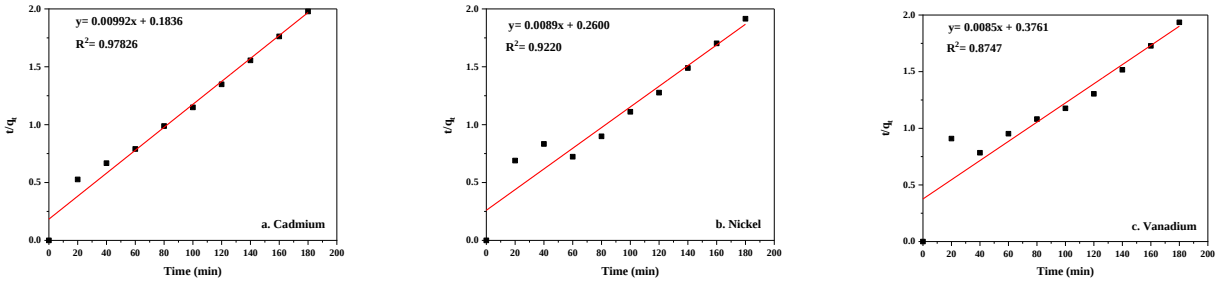

Fig. 8. Pseudo Second Order Kinetic Model of GO for (a. Cadmium, b. Nickel, and c. Vanadium) Adsorption

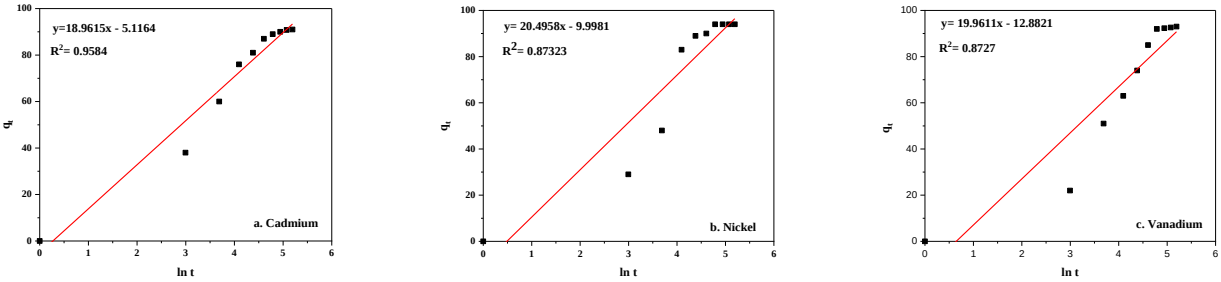

Fig. 9. Elovich Kinetic Model of GO for (a. Cadmium, b. Nickel, and c. Vanadium) Adsorption

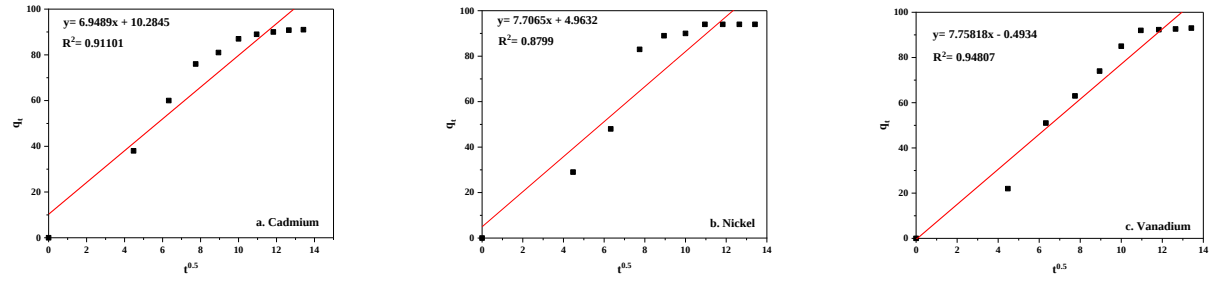

Fig. 10. Intra-Particle Diffusion Kinetic Model of GO for (a. Cadmium, b. Nickel, and c. Vanadium) Adsorption

3.4. Adsorption Thermodynamic Study

The values of thermodynamic functions, which are vital in defining many processes, notably the adsorption process, may be used to understand the types of driving forces and the reaction's direction. Additionally, they provide a convincing justification for the uniformity of molecules in diverse systems as a consequence of numerous molecular manipulations. The Gibbs free energy (ΔG) is the function that determines whether the reaction or change is spontaneous or not. The value of enthalpy (ΔH) represents a straightforward measurement of the interference forces between the adsorbed particle and the surface of the adsorbent, while the value of

entropy (ΔS) represents a measure of the anarchism and randomness of the molecules on the adsorption surface. The Van't Hoff relation Equation (15), which was developed by Dutch scientist Jacobus Henricus Van't Hoff in 1884, might be used to calculate the thermodynamic variables.

$$lnk_{ad} = -\frac{\Delta H}{R}\frac{1}{T} + \frac{\Delta S}{R} \quad (15)$$

Where k_{ad}: Adsorption thermodynamic equilibrium coefficient (dimensionless), R: universal gas constant (8.3144 J mol^{-1} K^{-1}), T: Absolute temperature (K), ΔH: Enthalpy change (J mol^{-1}), and ΔS: the Entropy change (J mol^{-1} K^{-1}).

Equation (16) calculates the adsorption thermodynamic equilibrium coefficient.

$$k_{ad} = \frac{q_e}{c_e} \quad (16)$$

By plotting the relation between lnk_{ad} and $\frac{1}{T}$, it gives a straight line of slope represented by ΔH and ΔS can be calculated from the intercept.

Equation (17) below may be used to get the system's Gibbs free energy (G):

$$\Delta G = \Delta H - T\Delta S \quad (17)$$

Fig. **11** show the outcomes of the thermodynamic analysis, and tables that give the values of the thermodynamic functions are listed in Table **4**.

It is well known that the thermodynamic functions (ΔH, ΔS, ΔG) are essential for figuring out the spontaneous process and describing how metal ions adsorb on the surface of adsorbent media. On the other hand, this method may be used to precisely characterize the situation of interference between the two surfaces of the solid phase and the liquid phase.

According to the obtained information from the figures and tables above showing the adsorption process of Cd, Ni, and V metals on the surface of GO, the thermodynamic equilibrium coefficient k_{ad} is demonstrated to decrease with rising Temperature t. This might be because when the temperature is elevated, the bond between the ions of the adsorbent metals and the active sites on the adsorption surface breaks, allowing the ions to be freed and reintroduced into the solution.

The enthalpy function's values that influenced ΔH, were all negative. This figure indicates the process of investigating the exothermic adsorption of heavy metal ions on surfaces of adsorption materials.

Chemical adsorption causes GO to absorb Cd, Ni, and V (chemisorption). An augmentation of interaction between the adsorbed metal ions and the adsorption surface as a result of a chemical reaction and the formation of a new type of electronic bonds with the functional groups on the surface of the adsorbent material are both indicated by an enthalpy value greater than 40 (kJ mol^{-1}).

The negative value of the entropy function changing ΔS for all adsorption tests using all the utilized adsorbent materials illustrates the reduction in randomness state in the surface overlap between the solid phase and the liquid phase throughout the adsorption process. This number also represents the three heavy metal ions' surface affinities for adsorption from the solution. Because the entropy function has a negative value during the adsorption process, the molecules are dispersed more evenly than they are while they are in solution. As a consequence of the exchange of heavy metal ions with less mobile ions on the surface of the material, entropy is reduced during the adsorption process.

Additionally, it was shown that under the experimental conditions investigated, where the values of Gibbs free energy changing ΔG were negative, the process of adsorption for heavy metal ions examined using adsorption materials is spontaneous.

This suggests that the Cd, Ni, and V ion adsorption on the adsorption sites in the adsorbent GO is an energy-free spontaneous process. Additionally, the fact that the negative value of compressive energy decreases as system temperature rises suggests that spontaneity decreases and that adsorption favor colder temperatures.

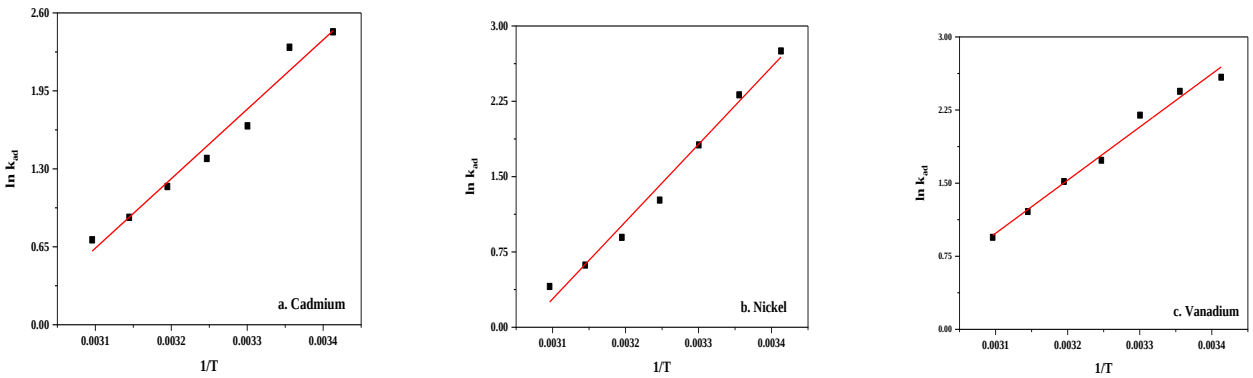

Fig. 11. Thermodynamic Behaviors of (a. Cadmium, b. Nickel, and c. Vanadium) Adsorption Using GO

Table 4. Thermodynamic Behaviors of Cadmium, Nickel, and Vanadium Adsorption Using GO

Metal	Temperature, (°C)	Alteration of Enthalpy ΔH, (kJ.mol^{-1})	Alteration of Entropy ΔS, (J.mol^{-1}. K^{-1})	Alteration of Gibbs free Energy ΔG, (kJ.mol^{-1})
Cd^{+2}	20	-48.1719	-144.0284	-5.9498
	25			-5.7325
	30			-4.1775
	35			-3.5501
	40			-2.9997
	45			-2.3674
	50			-1.90187
Ni^{+2}	20	-63.9944	-196.0374	-6.7031
	25			-5.7325
	30			-4.5732
	35			-3.2412
	40			-2.3302
	45			-1.6367
	50			-1.0889
V^{+5}	20	-45.3358	-132.3480	-6.3015
	25			-6.0514
	30			-5.5354
	35			-4.4420
	40			-3.9462
	45			-3.19475
	50			-2.5364

4- Conclusions

To create Nano Graphene Oxide (GO) from graphite powder in this work, the Hummers process was modified. Metal ions' enhanced ability to bind to GO is owing to their characteristics of hydrophilic and the oxygen-containing functional group's presence. Since they share an electron pair, these groups may effectively bind metal ions to create metal complexes. The removal efficiency of all metal ions rose as the temperature decreased, reaching a maximum of 20 °C and declining to 50 °C. when the initial Cd, Ni, and V concentration is 100 (mg L^{-1}) The concentrations of equilibrium values were, respectively, 8.9, 4.9, and 6.9 (mg L^{-1}). For all heavy metal ions as the initial concentration value increases for adsorbent metals, the percentage removal decreases. The Langmuir model may be explained by the adsorption isotherms; they show that heavy metal ions adsorb on monolayer-coated GO graphene sheets. Since it was fitted, the kinetic analysis implies that chemical adsorption (chemisorption), Metal ion adsorption on GO is regulated by the complexation of the surface for heavy metal ions containing oxygen groups on the GO surface. For Cd, and Ni ion to the pseudo-second-order kinetic model, and V ion to Intra-particle diffusion. The thermodynamic equilibrium coefficient k_{ad} for the adsorption of Cd, Ni, and V ions declines with increasing temperature *t*, and the values of the enthalpy function ΔH are negative, suggesting that the process is exothermic. A negative entropy function, ΔS, causes the reduction in randomness. In addition, the adsorption material ions were spontaneous, with negative Gibbs free energy values influencing ΔG.

References

[1] D. K. Tiku, A. Kumar, S. Sawhney, V. P. Singh, and R. Kumar, "Effectiveness of Treatment Technologies for Wastewater Pollution Generated by Indian Pulp Mills," *Environ Monit Assess*, vol. 132, no. 1–3, pp. 453–466, Sep. 2007.

[2] H. M. Rashid and A. A.H. Faisal, "Removal of Dissolved Cadmium Ions from Contaminated Wastewater using Raw Scrap Zero-Valent Iron and Zero Valent Aluminum as Locally Available and Inexpensive Sorbent Wastes," *IJCPE*, vol. 19, no. 4, pp. 39–45, Dec. 2018, doi: 10.31699/IJCPE.2018.4.5.

[3] I. Y. El-Sherif, S. Tolani, K. Ofosu, O. A. Mohamed, and A. K. Wanekaya, "Polymeric nanofibers for the removal of Cr(III) from tannery waste water," *Journal of Environmental Management*, vol. 129, pp. 410–413, Nov. 2013, doi: 10.1016/j.jenvman.2013.08.004.

[4] D. Gola, A. Malik, Z. A. Shaikh, and T. R. Sreekrishnan, "Impact of Heavy Metal Containing Wastewater on Agricultural Soil and Produce: Relevance of Biological Treatment," *Environ. Process.*, vol. 3, no. 4, pp. 1063–1080, Dec. 2016, doi: 10.1007/s40710-016-0176-9.

[5] M. Taseidifar, F. Makavipour, R. M. Pashley, and A. F. M. M. Rahman, "Removal of heavy metal ions from water using ion flotation," *Environmental Technology & Innovation*, vol. 8, pp. 182–190, Nov. 2017, doi: 10.1016/j.eti.2017.07.002.

[6] I. Demiral, C. Samdan, and H. Demiral, "Enrichment of the surface functional groups of activated carbon by modification method," *Surfaces and Interfaces*, vol. 22, p. 100873, Feb. 2021, doi: 10.1016/j.surfin.2020.100873.

[7] W. Zeng, W. Guo, B. Li, Z. Wei, D. D. Dionysiou, and R. Xiao, "Kinetics and mechanistic aspects of removal of heavy metal through gas-liquid sulfide precipitation: A computational and experimental study," *Journal of Hazardous Materials*, vol. 408, p. 124868, Apr. 2021.

[8] H. Khani, M. K. Rofouei, P. Arab, V. K. Gupta, and Z. Vafaei, "Multi-walled carbon nanotubes-ionic liquid-carbon paste electrode as a super selectivity sensor: Application to potentiometric monitoring of mercury ion(II)," *Journal of Hazardous Materials*, vol. 183, no. 1–3, pp. 402–409, Nov. 2010.

[9] T. A. Saleh and V. K. Gupta, "Synthesis and characterization of alumina nano-particles polyamide membrane with enhanced flux rejection performance," *Separation and Purification Technology*, vol. 89, pp. 245–251, Mar. 2012, doi: 10.1016/j.seppur.2012.01.039.

[10] A. E. Burakov *et al.*, "Adsorption of heavy metals on conventional and nanostructured materials for wastewater treatment purposes: A review," *Ecotoxicology and Environmental Safety*, vol. 148, pp. 702–712, Feb. 2018, doi: 10.1016/j.ecoenv.2017.11.034.

[11] Basma Abbas Abdel Majeed, Raheem Jameel Muhseen, and Nawras JameelJassim, "Adsorption of Diclofenac Sodium and Ibuprofen by Bentonite Polyureaformaldehyde Thermodynamics and Kinetics Study," *Iraqi Journal of Chemical and Petroleum Engineering*, vol. 19, no. 1, pp. 29–43, Mar. 2018.

[12] X. Wang *et al.*, "Synthesis of novel nanomaterials and their application in efficient removal of radionuclides," *Sci. China Chem.*, vol. 62, no. 8, pp. 933–967, Aug. 2019, doi: 10.1007/s11426-019-9492-4.

[13] C. Guerrero-Fajardo, L. Giraldo, and J. Moreno-Piraján, "Preparation and Characterization of Graphene Oxide for Pb(II) and Zn(II) Ions Adsorption from Aqueous Solution: Experimental, Thermodynamic and Kinetic Study," *Nanomaterials*, vol. 10, no. 6, p. 1022, May 2020, doi: 10.3390/nano10061022.

[14] Q. Kong *et al.*, "Relations between metal ion characteristics and adsorption performance of graphene oxide: A comprehensive experimental and theoretical study," *Separation and Purification Technology*, vol. 232, p. 115956, Feb. 2020, doi: 10.1016/j.seppur.2019.115956.

[15] W. S. Hummers and R. E. Offeman, "Preparation of Graphitic Oxide," *J. Am. Chem. Soc.*, vol. 80, no. 6, pp. 1339–1339, Mar. 1958, doi: 10.1021/ja01539a017.

[16] C. Bulin *et al.*, "Magnetic graphene oxide nanocomposite: One-pot preparation, adsorption performance and mechanism for aqueous Mn(II) and Zn(II)," *Journal of Physics and Chemistry of Solids*, vol. 156, p. 110130, Sep. 2021, doi: 10.1016/j.jpcs.2021.110130.

[17] J. Chen, B. Yao, C. Li, and G. Shi, "An improved Hummers method for eco-friendly synthesis of graphene oxide," *Carbon*, vol. 64, pp. 225–229, Nov. 2013, doi: 10.1016/j.carbon.2013.07.055.

[18] S. S. Türkaslan, Ş. S. Ugur, B. E. Türkaslan, and N. Fantuzzi, "Evaluating the X-Ray-Shielding Performance of Graphene-Oxide-Coated Nanocomposite Fabric," *Materials*, vol. 15, no. 4, p. 1441, Feb. 2022, doi: 10.3390/ma15041441.

[19] S. K. Tiwari, A. Huczko, R. Oraon, A. De Adhikari, and G. C. Nayak, "Facile electrochemical synthesis of few layered graphene from discharged battery electrode and its application for energy storage," *Arabian Journal of Chemistry*, vol. 10, no. 4, pp. 556–565, May 2017, doi: 10.1016/j.arabjc.2015.08.016.

[20] H. Li and Z. Wei, "Impacts of Modified Graphite Oxide on Crystallization, Thermal and Mechanical Properties of Polybutylene Terephthalate," *Polymers*, vol. 13, no. 15, p. 2431, Jul. 2021, doi: 10.3390/polym13152431.

[21] M. Parastar, S. Sheshmani, and S. Shokrollahzadeh, "Cross-linked chitosan into graphene oxide-iron(III) oxide hydroxide as nano-biosorbent for Pd(II) and Cd(II) removal," *International Journal of Biological Macromolecules*, vol. 166, pp. 229–237, Jan. 2021, doi: 10.1016/j.ijbiomac.2020.10.160.

[22] Zainab Jabbar Shadhan and Mohammed N. Abbas, "Removal of Heavy Metals from Refineries Wastewater," Master of Science in Environmental Engineering, Mustansiriyah University, Iraq, 2021.

[23] E. N. Mahmoud, F. Y. Fayed, K. M. Ibrahim, and S. Jaafreh, "Removal of Cadmium, Copper, and Lead from Water Using Bio-Sorbent from Treated Olive Mill Solid Residue," *Environmental Health Insights*, vol. 15, p. 117863022110531, Jan. 2021, doi: 10.1177/11786302211053176.

[24] D. K. Venkata Ramana, J. S. Yu, and K. Seshaiah, "Silver nanoparticles deposited multiwalled carbon nanotubes for removal of Cu(II) and Cd(II) from water: Surface, kinetic, equilibrium, and thermal adsorption properties," *Chemical Engineering Journal*, vol. 223, pp. 806–815, May 2013, doi: 10.1016/j.cej.2013.03.001.

[25] A. R. Kaveeshwar, S. K. Ponnusamy, E. D. Revellame, D. D. Gang, M. E. Zappi, and R. Subramaniam, "Pecan shell based activated carbon for removal of iron(II) from fracking wastewater: Adsorption kinetics, isotherm and thermodynamic studies," *Process Safety and Environmental Protection*, vol. 114, pp. 107–122, Feb. 2018, doi: 10.1016/j.psep.2017.12.007.

[26] D. J. O'Shannessy and D. J. Winzor, "Interpretation of Deviations from Pseudo-First-Order Kinetic Behavior in the Characterization of Ligand Binding by Biosensor Technology," *Analytical Biochemistry*, vol. 236, no. 2, pp. 275–283, May 1996, doi: 10.1006/abio.1996.0167.

النمذجة الرياضية والحركية لازالة ايونات المعادن من مياه مخلفات الصرف الصناعي

نزار عبد المهدي جواد و طارق محمد نايف

قسم الهندسة الكيمياوية/كلية الهندسة/ جامعة بغداد

الخلاصة

الهدف من الدراسة هو إنتاج نانو اوكسيد الجرافين (GO) لاستخدامه في عملية امتزاز الدفعات لازالة المعادن الثقيلة (الكادميوم Cd^{+2}، النيكل Ni^{+2}، والفاناديوم V^{+5}) من مياه مخلفات الصرف الصناعي. تمت دراسة تأثيركل من تغير درجة الحرارة (٢٠-٥٠) درجة مئوية وتغير التركيز الابتدائي (١٠٠-٨٠٠) ملغم / لتر على عملية الامتزاز. تم استخدام محلول مائي من الأيونات محاكي لعينات المخلفات لتحديد متساوي درجة حرارة الامتصاص (adsorption isotherms) ، وبعد جمع البيانات التجريبية، تمت دراسة عملية الامتصاص حركيًا وديناميكيًا حراريًا. تم استخدام نماذج متساوية الحرارة (adsorption isotherms): Langmuir و Freundlich و Temkin لتناسب البيانات، وأظهرت النتائج أن أيونات الكادميوم، النيكل والفاناديوم على سطح الامتصاص نانو اوكسيد الجرافين تتلائم مع نموذج Langmuir مع معاملات الارتباط (R^2) البالغة ٠,٩٩٩. أظهرت النماذج الحركية التي تمت دراستها أنه تم اتباع نموذج من الدرجة الثانية الزائفة وديناميكا حرارية، وكانت العملية طاردة للحرارة بسبب $H\Delta$ سالبة، وانخفاض العشوائية بسبب $S\Delta$ سالب. بالإضافة إلى ذلك، تأثر الامتزاز التلقائي لأيونات المعادن بقيم $G\Delta$ السلبية.

الكلمات الدالة: نانو أكسيد الجرافين، ايونات المعادن الثقيلة، مياه الصرف الصحي، نموذج لانموي، نموذج بسيدو الدرجة الثانية، دراسة الديناميكا الحرارية.